Atlas Journal of Materials Science 1 (1): 24–29, 2014
doi: 10.5147/ajms.2014.0171

Innovative Nanoimprint-Assisted Fabrication of Anodic Aluminum Oxide

Po-Chun Chen[1], Youwei Jiang[1], Dawen Li[2], Jun Zou[1], and Xing Cheng[3*]

[1] Department of Electrical Engineering, Texas A&M University, College Station, TX 77843-3128, USA;
[2] Department of Electrical and Computer Engineering, University of Alamama, Tuscaloosa, AL 35487, USA;
[3] Department of Material Science and Engineering, South University of Science and Technology of China, Shenzhen, Guangdong 518055, China.

Received: June 7, 2014 / Accepted: June 17, 2014

Abstract

Anodic aluminum oxide (AAO) templates possess highly-ordered nanoporous structures, with advantages such as high aspect ratio. However, there are limits to control the growth of the traditional AAO arrays, such as interpore distance, pore sizes and densities. In this study, we introduce an innovative nanoimprint process guided AAO fabrication to overcome these limitations of the traditional AAO arrays.

Keywords: Nanoimprint, controllable anodic aluminum oxide template.

* Corresponding author: chengx@sustc.edu.cn

Introduction

Anodic aluminum oxide (AAO) template possesses nanoporous structures, with advantages of high aspect ratio, highly-ordered, uniform and controllable pore size (from 10 nm to 500 nm), and stability in chemical and thermal surroundings. In the last decade, AAO nanoporous structures with naturally self-ordered nanotubes have been extensively investigated as an important assisting material. For instance, magnetic (Whitney et al., 1993), electronic (Stucky and Macdougall, 1990), optoelectronic (Beck et al., 1992), biological (Matsumoto et al., 2005), and micromechanical devices (Masuda et al., 1997) can be effectively fabricated by using AAO as templates.

There are, however, limits to control the AAO growth. The long-range self-assembled nanostructure can only been observed under certain anodization conditions with specific dilute acidic solutions (sulfuric acid, oxalic acid, or phosphoric acid). AAO nanoporous is a self-ordered structure, with nanopore locations generated randomly in a hexagonal close-packed pattern. Secondary anodization is a method to fabricate near defect-free AAO templates, and it creates a pattern through removing the previously anodized layer. Such a pattern helps to form the AAO structure based on those nanoindents in a bowl shape (Chen et al., 2005; Chen et al., 2012; Montero et al., 2014). Influenced by this concept, many research studies focus on the pretreated aluminum and attempt to control the locations of nanopores. Lee's group used a traditional photolithography fabrication to replicate a nickel imprint stamp with a defect-less hexagonal pattern in order to produce an ideal AAO nanoporous

Atlas Journal of Materials Science - ISSN 2330-6831. Published By Atlas Publishing, LP (www.atlas-publishing.org)

structure (Lee and Lee, 2010). Focus ion-beam lithography (Liu et al., 2001), scanning probe microscopic lithography (Masuda et al., 2002), optical diffraction grating (Mikulskas et al., 2001), and microbeads (Masuda et al., 2004; Surawathanawises and Cheng, 2014) have been investigated as pretreatments of aluminum. However, these fabrication processes are relatively slow and expensive. In light of all alternatives, nanoimprint method seems to be a promising technique to pre-pattern with high-yield results at a low cost (Lee et al., 2006). Chung's group fabricated square-array AAO nanopores on Si assisted by nanoimprint (Kwon et al., 2009). Choi et al. reported that nanoimprinted pre-pattern can change the nanopore distance from the lattice constant (Choi et al., 2005). Furthermore, Jin's group not only fabricated long-range location controllable AAO, but also created different sizes of nanopores on the same aluminum substrate with nanoimprint-guided anodization (Noh et al., 2010).

In this study, we designed nanoimprint molds with different orders, pillar size and inter-distance to investigate how to control the location to form AAO nanopores. Moreover, growing various sizes of nanopores can be conducted with the assistance from the nanoimprint. Therefore, fabricating AAO with different nanopores on the same aluminum piece can be performed.

Materials and Methods

A pure Al piece (99.999%) was refined and smoothened by mechanical polishing and electrochemical polishing in order to prevent any possible defects which may affect the nanoimprint process. The Al piece was first mechanically refined and polished, and then annealed at 400 ^{0}C for 30 min to relieve residual stresses. The electropolishing was conducted in an electrolyte of 15 vol.% perchloric acid (HC_1O_4), 70 vol.% ethanol (C_2H_5OH)

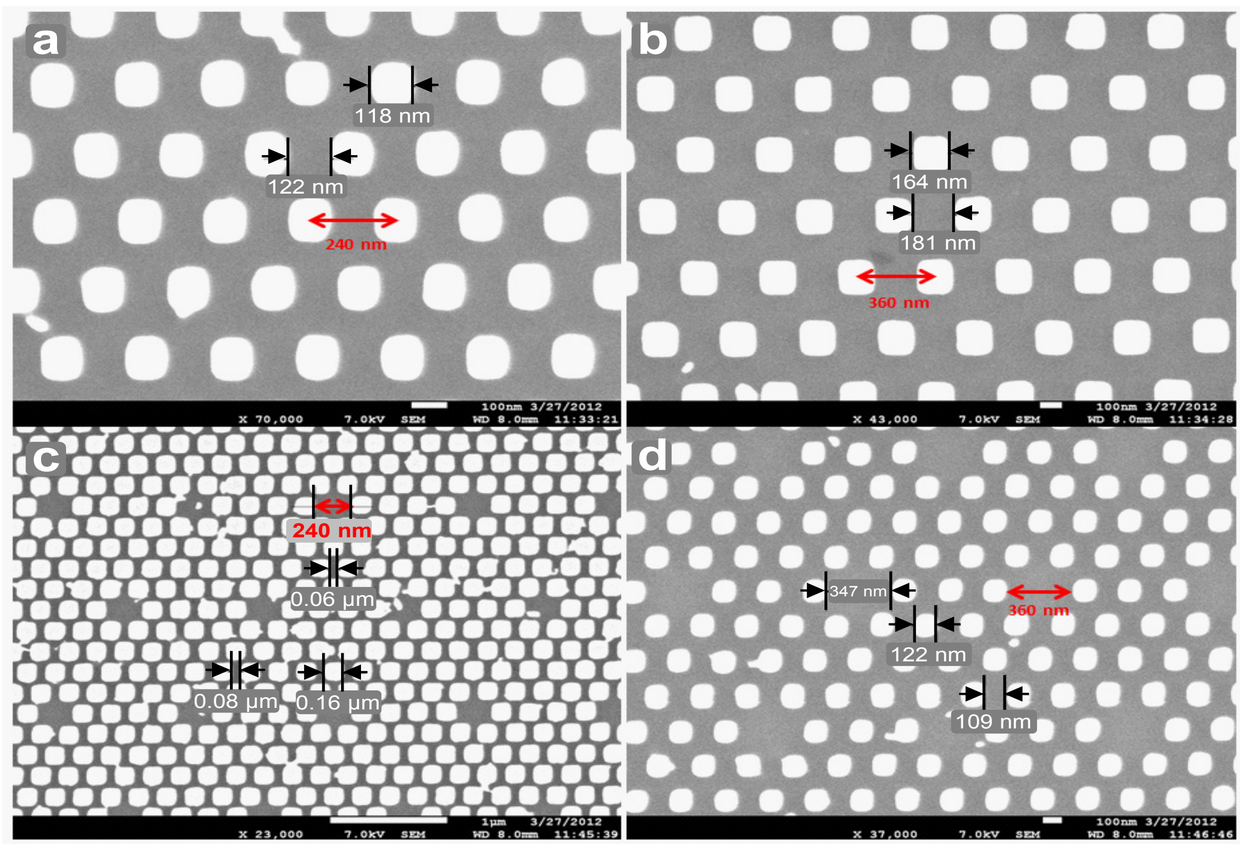

Figure 1. SEM images of imprinting mold, with pillar size of 120 nm and inter-distance of 240 nm (a); pillar size of 160 nm and inter-distance of 360 nm (b); vacancy size of 240 nm (c); and vacancy size of 360 nm (d).

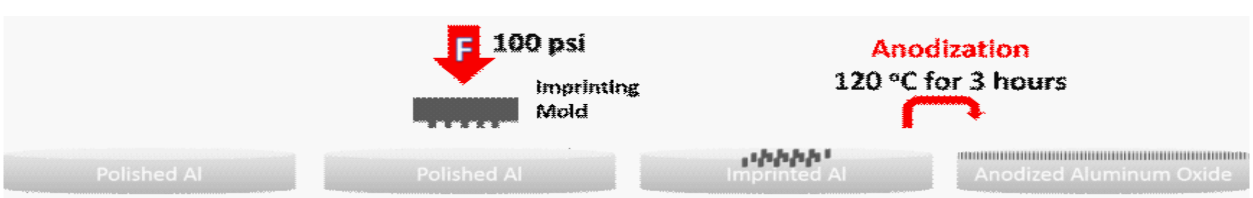

Figure 2. Schematic diagram of the entire fabrication process.

and 15 vol.% butyl cellosolve ($CH_3(CH_2)_3OCH_2CH_2OH$) solution, with 40 V applied voltage at 5 ^{0}C for 10 min.

The nanoimprint mold was designed as hexagonal arrays of pillars with different orders, pillar sizes, and inter-distances. Fig. 1 shows SEM images of the imprint mold. The pillar sizes are either ~160 or ~120 nm, with their inter-distances of ~360 or ~240 nm, respectively (Fig. 1 a and b). There are also some designed vacancies on the imprinting mold, and the open sizes are either ~360 nm or ~240 nm, respectively (Fig. 1 c and d). The electropolished Al piece was directly indented by the designed imprinting mold with a pressure of 100 psi. The nanoimprinted aluminum piece was anodized at 120 V in a 1 vol.% phosphoric acid (H_3PO_4) solution at 0 ^{0}C for 3 hours. Fig. 2 shows the schematic diagram of the entire fabrication process. The microstructures of the specimens were analyzed by field-emission scanning electron microscopes (SEM), FEI Quanta 600 and JEOL JSM-7500.

Results and Discussion

In order to fabricate a nanoimprinted aluminum piece, a very flat surface is crucial. To indent an aluminum substrate at the nanometer scale accuracy, a surface roughness of even a few nanometers is undesirable. Fig. 3 shows optical microscopic (OM) images of electropolished aluminum pieces. Fig. 3(a) is an image of an un-annealed aluminum piece after electropolishing, while Fig. 3(b), an annealed one. The grain size in Fig. 3(a) is much smaller than that in Fig. 3(b). Since grain boundaries are considered as defects on the aluminum piece for nanoimprinting, annealing not only relieves residual stresses, but also drives crystal growth to enlarge the grains with reduced grain boundaries, or fewer defects. The grains in Fig. 3(b) are much larger than the nanoimprinting pattern regime, so the aluminum piece is suitable for nanoimprinting.

Fig. 4 shows SEM images of imprinted patterns, with 160 nm pillars while some of them are replaced with 120 nm pillars. The substituted smaller pillars are shown in every three pillars in Fig. 4(a), while in every four pillars in Fig. 4(b). Anodizing voltage has a direct effect on the pore size (Belwalkar et al., 2008), and normally nanopores are around 120 nm in diameter at 120 V using H_3PO_4 solution. The results shown in Fig. 4 indicate that AAO only forms with 120 nm indentations (marked with red circles). On the other hand, the 160 nm indentations were too large to grow single pores, so more nanotubes could form in a single 160 nm indentation. Therefore, the location of AAO can be controlled by a pattern with similar size of the AAO nanopores on aluminum before anodizing. Fig. 5 shows SEM images of anodization results with differently designed patterns, demonstrating the possibility to alternate the locations of nanopores. Fig. 5(a) shows smaller indentations (120 nm) surrounded by larger ones, while in Fig. 5(b), larger pores surrounded by smaller ones. More importantly, these AAO samples contain pores with different sizes on the same piece of aluminum, which are impossible to obtain by the traditional AAO fabrication. Fig. 6 shows SEM images of anodization results with another designed pattern, which includes vacancies in the hexagonal array (Fig. 1c). There were two types of AAO nanopores. Fig. 6(a) is a SEM image of AAO arrays with a vacancy inserted in every three indentations, while in Fig. 6(b), a vacancy in every four indentations. This type of design demonstrated that the indentation with suitable size is able to drive AAO to form a desired shape, while on a flat surface without indentation, AAO forms as irregular shapes, as shown in Fig. 6(a) and (b). Therefore, producing vacancies is another promising design to obtain nanopores with different sizes on a single piece of aluminum.

Fig. 7 is a schematic diagram of the relationship between the nanoimprinted patterns and the anodic nanopores based on the imprinted dents. Fig. 7(a) shows the imprinted dents on the Al surface after nanoimprinting, and Fig 7(b) is the anodized results with different possible patterns. Overall, proper pattern designs can lead to the formation of nanopores at given locations to obtain ideal shapes of the AAO nanopores. However, aluminum with large imprinted pattern, or without imprinted pattern, still need to undergo two-step anodization to acquire anodic nanopores with fine shapes.

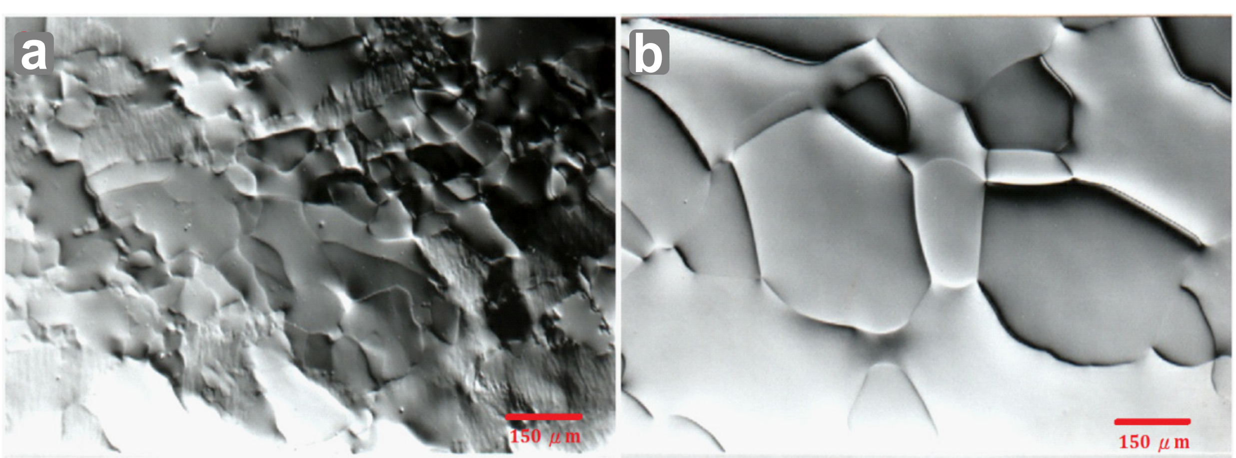

Figure 3. Optical microscopic images of electropolished Al from un-annealed (a) and annealed (b) Al pieces.

Atlas Journal of Materials Science - ISSN 2330-6831. Published By Atlas Publishing, LP (www.atlas-publishing.org)

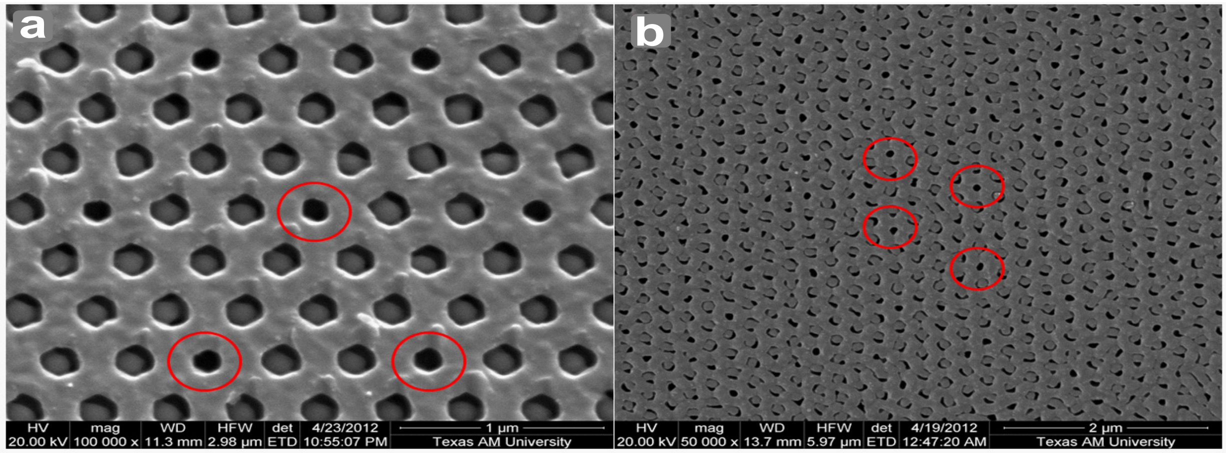

Figure 4. SEM images of imprinted indentation pattern with 160 nm and 120 nm pillars. Smaller pillars appear in every 3 larger pillars (a), or in every 4 larger pillars (b).

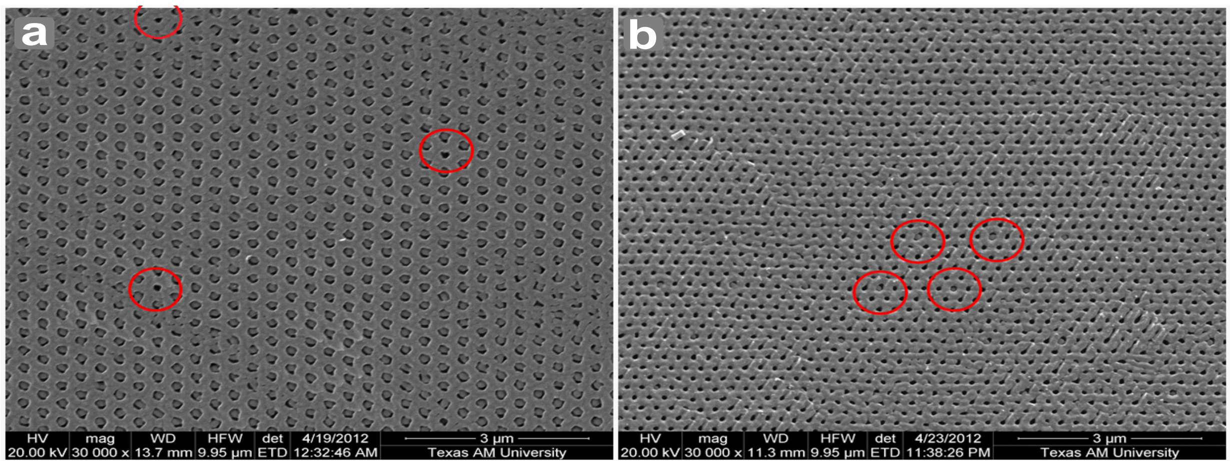

Figure 5. SEM images of AAO grown from different imprinted patterns. Smaller indentations surrounded by larger ones (a), and large indentations surrounded by smaller ones (b).

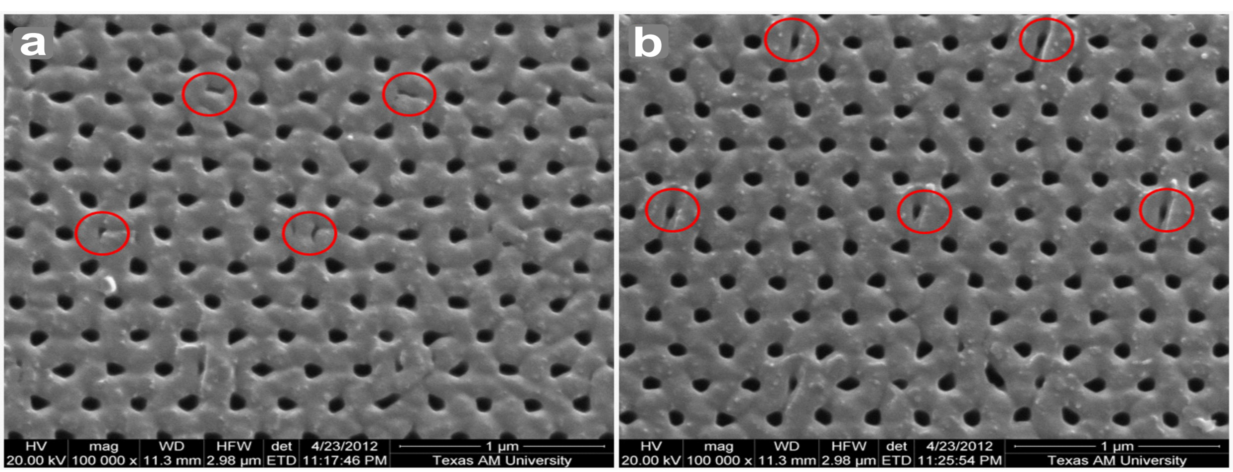

Figure 6. SEM images of AAO with vacancies introduced into patterns in every 3 indentations (a), or in every 4 indentations (b).

Atlas Journal of Materials Science - ISSN 2330-6831. Published By Atlas Publishing, LP (www.atlas-publishing.org)

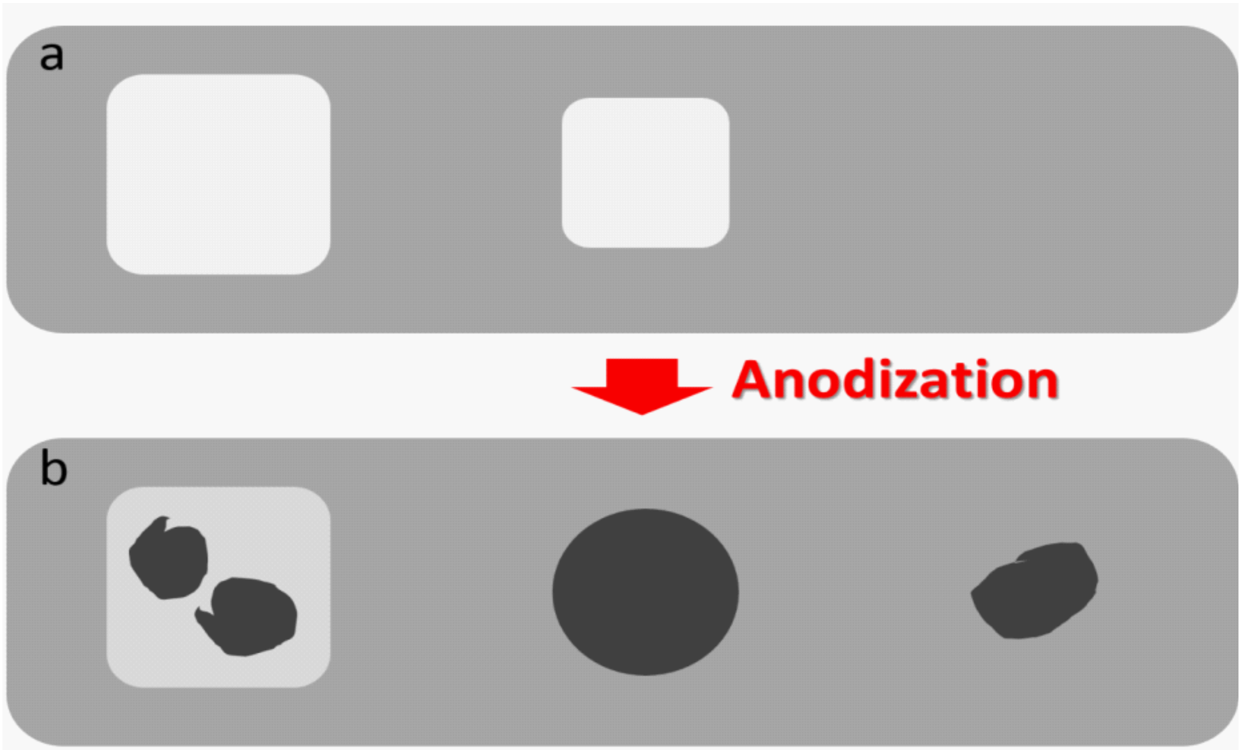

Figure 7. Schematic diagram of the relationship between the nanoimprinted patterns (a) and anodic nanopores (b).

Conclusions

In summary, AAO arrays were formed through a guided anodization assisted by a nanoimprinting process. We designed nanoimprinting patterns followed by AAO growth to form ordered hexagonal arrays with different pore sizes. We directly imprinted the designed patterns onto well-polished Al pieces. The guided anodization process controlled the nanopore locations, and more importantly, periodically ordered AAO arrays with different nanopore sizes could be fabricated. This study demonstrates an innovative AAO fabrication process to overcome the limitations of traditional AAO arrays. Further developments will be needed to include: (1) design of other nanoimprinting patterns for more specific applications; (2) introducing other fabrication processes to further control the pores density; and (3) introducing the results in this study for specific electronic, magnetic, or biological applications.

References

Beck JS, JC Vartuli, WJ Roth, ME Leonowicz, CT Kresge, KD Schmitt, CTW Chu, DH Olson, EW Sheppard, SB McCullen, JB Higgins and JL Schlenker (1992) A new family of mesoporous molecular-sieves prepared with liquid-crystal templates. Journal of the American Chemical Society 114 (27): 10834-10843.

Belwalkar A, E Grasing, W Van Geertruyden, Z Huang and WZ Misiolek (2008) Effect of processing parameters on pore structure and thickness of anodic aluminum oxide (AAO) tubular membranes. Journal of Membrane Science 319 (1-2): 192-198.

Chen CC, JH Chen and CG Chao (2005) Post-treatment method of producing ordered array of anodic aluminum oxide using general purity commercial (99.7%) aluminum. Japanese Journal of Applied Physics Part 1-Regular Papers Brief Communications & Review Papers 44 (3): 1529-1533.

Chen CC, D Fang, and Z Luo (2012) Fabrication and Characterization of Highly-Ordered Valve-Metal Oxide Nanotubes and Their Derivative Nanostructures. Reviews in Nanoscience and Nanotechnology 1(4): 229-256.

Choi J, RB Wehrspohn, and U Gosele (2005) Mechanism of guided self-organization producing quasi-monodomain porous alumina. Electrochimica Acta 50 (13): 2591-2595.

Kwon N, K Kim, J Heo, and I Chung (2009) Fabrication of ordered anodic aluminum oxide with matrix arrays of pores using nanoimprint." Journal of vacuum science & technology. A. Vacuum, surfaces, and films 27 (4): 803-807.

Lee J and J Lee (2010) Ideally Ordered Anodic Aluminum Oxide Membranes via the Replicated Nickel Imprint Stamp." Advanced Science Letters 3 (4): 411-414.

Lee W, R Ji, CA Ross, U Gosele, and K Nielsch (2006) Wafer-scale Ni imprint stamps for porous alumina membranes based on interference lithography. Small 2 (8-9): 978-982.

Liu CY, A Datta, and YL Wang (2001) Ordered anodic alumina nanochannels on focused-ion-beam-prepatterned aluminum surfaces. Applied Physics Letters 78 (1): 120-122.

Masuda H, F Hasegwa, and S Ono (1997) Self-ordering of cell arrangement of anodic porous alumina formed in sulfuric acid solution. Journal of the Electrochemical Society 144 (5): L127-L130.

Masuda H, K Kanezawa, and K Nishio (2002) Fabrication of ideally ordered nanohole arrays in anodic porous alumina based on nanoindentation using scanning probe microscope. Chemistry Letters (12): 1218-1219.

Masuda H, Y Matsui, M Yotsuya, F Matsumoto, and K Nishio (2004) Fabrication of highly ordered anodic porous alumina using self-organized polystyrene particle array. Chemistry Letters 33 (5): 584-

585.
Matsumoto F, M Harada, K Nishio, and H Masuda (2005) Nanometer-scale patterning of DNA in controlled intervals on a gold-disk array fabricated using ideally ordered anodic porous alumina. Advanced Materials 17 (13): 1609-1612.
Mikulskas I, S Juodkazis, R Tomasiunas, and JG Dumas (2001) Aluminum oxide photonic crystals grown by a new hybrid method. Advanced Materials 13 (20): 1574-1577.
Montero Moreno JM, M Waleczek, S Martens, R Zierold, D Görlitz, VV Martínez, VM Prida, and K Nielsch (2014) Constrained Order in Nanoporous Alumina with High Aspect Ratio: Smart Combination of Interference Lithography and Hard Anodization. Advanced Functional Materials 24 (13): 1857-1863.
Noh K, C Choi, JY Kim, Y Oh, KS Brammer, MC Loya, and SH Jin (2010) Long-range ordered aluminum oxide nanotubes by nano-imprint-assisted aluminum film surface engineering. Journal of Vacuum Science & Technology B 28 (6): C6M88-C86M92.
Stucky GD and JE Macdougall (1990) Quantum confinement and host guest chemistry - Probing a new dimension. Science 247 (4943): 669-678.
Surawathanawises K and X Cheng (2014) Nanoporous anodic aluminum oxide with a long-range order and tunable cell sizes by phosphoric acid anodization on pre-patterned substrates. Electrochimica Acta 117 (0): 498-503.
Whitney TM, JS Jiang, PC Searson, and CL Chien (1993) Fabrication and magnetic-properties of arrays of metallic nanowire. Science 261(5126): 1316-1319.

Atlas Journal of Materials Science - ISSN 2330-6831. Published By Atlas Publishing, LP (www.atlas-publishing.org)